

Accepted Manuscript

A western boundary current eddy characterisation study

Joachim Ribbe, Daniel Brieva

PII: S0272-7714(16)30533-9

DOI: [10.1016/j.ecss.2016.10.036](https://doi.org/10.1016/j.ecss.2016.10.036)

Reference: YECSS 5295

To appear in: *Estuarine, Coastal and Shelf Science*

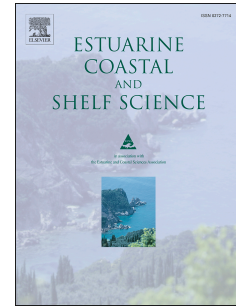
Received Date: 27 May 2016

Revised Date: 25 October 2016

Accepted Date: 26 October 2016

Please cite this article as: Ribbe, J., Brieva, D., A western boundary current eddy characterisation study, *Estuarine, Coastal and Shelf Science* (2016), doi: 10.1016/j.ecss.2016.10.036.

This is a PDF file of an unedited manuscript that has been accepted for publication. As a service to our customers we are providing this early version of the manuscript. The manuscript will undergo copyediting, typesetting, and review of the resulting proof before it is published in its final form. Please note that during the production process errors may be discovered which could affect the content, and all legal disclaimers that apply to the journal pertain.



1
2
3
4
5
6
7
8
9
10
11
12
13
14
15
16
17
18
19
20
21
22
23
24
25

A Western Boundary Current Eddy Characterisation Study

by

Joachim Ribbe and Daniel Brieva

International Centre for Applied Climate Sciences (ICACS), University of Southern Queensland,
Toowoomba 4350 Queensland, Australia

Corresponding author: Joachim.Ribbe@usq.edu.au

Manuscript for *Estuarine Coastal Shelf Science*

October 25, 2016

26

27

28 Key Points:

29

30 • 497 short-lived eddies detected in a coastal corridor off eastern Australia.

31

32 • About 23 individual short-lived eddies traced per year.

33

34 • 43% of cyclonic eddies (4-5 per year) found off southeast Queensland.

35

36 • Cyclonic eddies displaced shelf water by about 110-120 km.

37

38 • Cyclonic eddies postulated to establish quasi-permanent northward flow.

39

40 Abstract

41

42 The analysis of an eddy census for the East Australian Current (EAC) region yielded a
43 total of 497 individual short-lived (7-28 days) cyclonic and anticyclonic eddies for the
44 period 1993 to 2015. This was an average of about 23 eddies per year. 41% of the
45 tracked individual cyclonic and anticyclonic eddies were detected off southeast
46 Queensland between about 25 °S and 29 °S. This is the region where the flow of the
47 EAC intensifies forming a swift western boundary current that impinges near Fraser
48 Island on the continental shelf. This zone was also identified as having a maximum in
49 detected short-lived cyclonic eddies. A total of 94 (43%) individual cyclonic eddies or
50 about 4-5 per year were tracked in this region. The census found that these potentially
51 displaced entrained water by about 115 km with an average displacement speed of
52 about 4 km per day. Cyclonic eddies were likely to contribute to establishing an on-
53 shelf longshore northerly flow forming the western branch of the Fraser Island Gyre
54 and possibly presented an important cross-shelf transport process in the life cycle of
55 temperate fish species of the EAC domain. In-situ observations near western
56 boundary currents previously documented the entrainment, off-shelf transport and
57 export of near shore water, nutrients, sediments, fish larvae and the renewal of inner
58 shelf water due to short-lived eddies. This study found that these cyclonic eddies
59 potentially play an important off-shelf transport process off the central east Australian
60 coast.

61

62

63 **Keywords:** Western boundary currents; fisheries; eddies; transport; shelf dynamics;
64 East Australian Current.

65 1. Introduction

66

67 In-situ observations from Western Boundary Current (WBC) regions indicate that
68 cyclonic eddies (CEs) are important for fisheries (Kasai et al. 2002, Govoni et al.
69 2009, Suthers et al. 2011, Matis et al. 2014, Mullaney et al. 2014, and Everett et al.
70 2015). Forming on the near-coast side of WBC regions, CEs become enriched in fish
71 larvae and primary productivity stimulating nutrients due to the entrainment of near-
72 shore coastal water. The East Australian Current (EAC) CEs observed to the south of
73 the EAC intensification zone (Ridgway and Dunn 2003) were found to be usually
74 short-lived (2-4 weeks). The eddies were more frequent and of smaller scale than
75 anticyclonic eddies (ACEs) and ranged in size from about 10 km to 100 km
76 (Mullaney and Suthers 2013; Everett et al. 2015). Observed CEs propagated close to
77 the coastal zone, often generated a near-shore northward flow (e.g. Huyer et al. 1988,
78 Roughen et al. 2011, Everett et al. 2011) and were located at the coastal side of the
79 EAC. CEs were also usually cold-core eddies, i.e. characterised by a negative sea
80 surface temperature anomaly (SSTa), and Chlorophyll-a (Chl-a) concentrations were
81 about twice than those observed for ACEs (e.g. Govoni et al., 2009, Suthers et al.
82 2011, Everett et al. 2011, Everett et al. 2014, Mullaney et al. 2014, Everett et al.
83 2015). Studies of EAC CEs are few and limited to the southern regions of the EAC
84 (e.g. Oke and Griffin 2010; Macdonald et al. 2016), which is referred to as the EAC
85 separation zone (Ridgway and Dunn 2003). This study aimed to provide a census for
86 short-lived eddies (7-28 days) along the east Australian coast with a particular focus
87 on CE off the coast of southeast Queensland. This region is part of the EAC
88 intensification region (Figure 1).

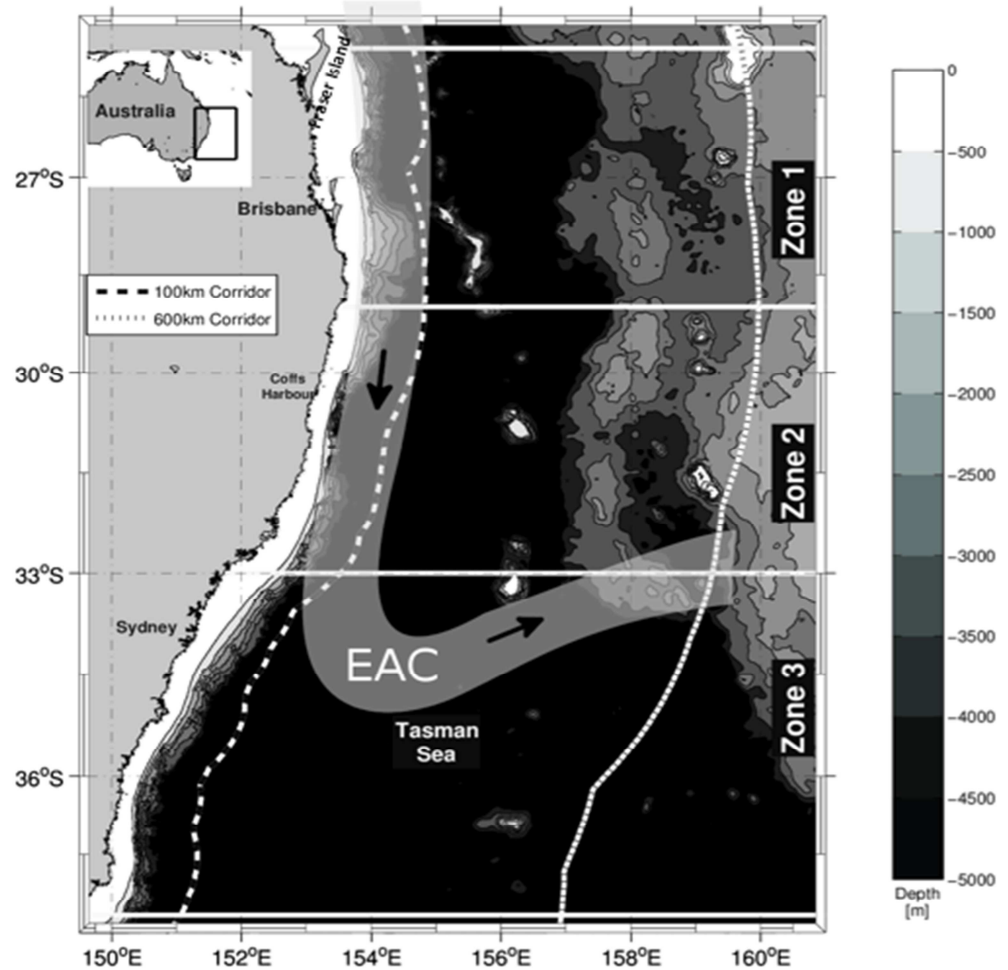
89

90 Everett et al. (2012) and Pilo et al. (2015) performed the only two eddy
91 characterisation studies of long-lived eddies (>28 days) for the EAC. Both studies
92 utilised data from the same global eddy census conducted by Chelton et al. (2011).
93 Pilo et al. (2015) compared the eddy statistics for three WBC regions, i.e. the Agulhas
94 Current, the Brazil Current and the EAC region. The study expanded on Everett et
95 al.'s (2012) analysis by estimating also average lifetime, propagation speed and
96 distance travelled. A census of short-lived CEs (7-28 days) propagating within close
97 proximity to the shelf, which appear to be more important for primary productivity
98 and fisheries due to the entrainment of near coast shelf water, recruitment and
99 retention is lacking for the EAC and other WBCs (Mullaney and Suthers 2013). The
100 analysis presented in this paper aimed to expand on these previous studies (Everett et
101 al. 2012, Pilo et al. 2015). Its focus was on the analysis of eddy characteristics
102 detected in a coastal corridor of about 100 km width, i.e. eddies that were wedged
103 between the coast line and the EAC. We quantified the occurrences of short-lived
104 cyclonic eddies important to fisheries and provided the first assessment of the role of
105 these eddies for the coastal ocean off southeast Queensland.

106

107 The east Australian continental shelf is at its widest (80-90 km) off the coast of
108 southeast Queensland between about 25-27 °S and to the south of Fraser Island
109 (Figure 1). The EAC forms to the north of this region from the South Equatorial
110 Current and Coral Sea outflows. It intensifies forming a swift, albeit seasonally
111 varying in strength, southward flowing current hugging the continental shelf
112 (Ridgway and Dunn, 2003). A prominent oceanographic feature of the region is the
113 EAC-driven Southeast Fraser Upwelling System (Brieva et al. 2015).

114



115

116

117 Figure 1: Location of the study site along the east coast of Australia. The boundaries
 118 (white lines) between Zone 1 (Z1) and Zone 2 (Z2) at about 29° S and Z2
 119 and Zone 3 (Z3) at about 33° S were identified in this study from minima
 120 in eddy activity. Approximate mean path of the East Australian Current
 121 (EAC) is shown in light grey. Eddies were tracked over the whole region.
 122 An eddy census was conducted and the analysis limited to two coastal
 123 corridors of 100 km and 600 km width each (dash lines).

124

125

126 Ward et al. (2003) and Mullaney et al. (2014) speculated that the northern sub-tropical
 127 shelf waters (~25-27 °S) of the EAC intensification zone supply larvae of temperate
 128 fish species that are transported southward with the EAC. These return at a later stage

129 in their lifecycle to spawn again during early winter. Gruber et al. (2011) find that
130 eddy induced transports appeared to be close to a maximum within a near-shore 100
131 km wide zone. Mullaney and Suthers (2013) argued for the importance of these near-
132 coast short-lived eddies for fisheries. The eddies were also found to be associated with
133 the northward countercurrent and entrainment of coastal waters (Huyer et al. 1988,
134 Mullaney and Suthers 2013). Thus, the analysis presented in this study was focused
135 on eddies and their characteristics identified for a narrow 100 km wide coastal
136 corridor (Figure 1). The characteristics were obtained from a new eddy census for the
137 southwestern Pacific Ocean using the Halo et al. (2014) eddy detection method. It led
138 to the identification of three zones (Zone 1 or Z1, Zone 2 or Z2 and Zone 3 or Z3)
139 distinguished from minima in eddy activity (Figure 1). Z1 was identified as the region
140 with the highest number of short-lived cyclonic eddies along the east coast of
141 Australia.

142

143 **2. Data and Methodology**

144

145 **2.1 Data**

146

147 Daily estimates of Chl-a ($\text{mg}\cdot\text{m}^{-3}$) and SST ($^{\circ}\text{C}$) were disseminated via the data portal
148 of Australian Integrated Marine Observing System (IMOS 2015a) and were used in
149 this study for the period 09/08/2002 to 31/10/2015. The data was gridded with a
150 spatial resolution of 0.01° (IMOS 2015a). The data was derived from MODerate
151 resolution Imaging Spectroradiometer (MODIS) measurements with methodological
152 details provided by O'Reilly et al. (2000) and Claustre and Maritorena (2003).

153

154 Gridded sea surface height anomaly (SSHa) was available for the period 01/01/1993 –
155 31/10/2015 and for every second day until 31/12/2010 and daily thereafter (IMOS
156 2015b). The eddy detection tool provided by Halo et al. (2014) was applied to SSHa
157 data for this period (Section 2.2 Methodology). The spatial resolution of SSHa data
158 used in this study was $1/5^{\circ}$. This compared to the $1/4^{\circ}$ resolution in Chelton et al.
159 (2011), which was evaluated by Everett et al. (2012) and Pilo et al. (2015) resolving
160 eddies with a minimum radii of >40 km and lifetime larger than 28 days. Halo et al.
161 (2014) used SSH gridded data with 0.25° resolution and tracked eddies with lifetime
162 larger than 30 days. Census data from the application of the Halo et al. (2014) method
163 in this study and for lifetimes of at least 7 days were presented in Table 1.

164

165 The mean eddy core characteristics such as Chl-a, SST and SSHa were determined for
166 all detected eddies (Table 2). The core size was defined in this study to have a radius
167 of 20 km. Chl-a and SST anomalies were also computed as the difference in mean
168 value for the core and the value computed for a larger area with radius of 40 km, but
169 excluding any values within the core. The number of observations to determine Chl-a
170 and SST anomalies was much reduced compared to SSHa data due to frequent and
171 extensive cloud coverage (see also discussion in Brieva et al. 2015).

172

173 **2.2 Methodology**

174

175 Methods to track eddies in remotely sensed observation of SSHa and ocean model
176 data were described by e.g. Chelton et al. (2007), Henson and Thomas (2007),
177 Chelton et al. (2011), Morrow and Le Traon (2012), Mason et al. (2014), Halo et al.
178 (2014), Karstensen et al. (2015), and Pegliasco et al. (2015). The eddy-tracking

179 algorithm utilised in this study was initially proposed by Penven et al. (2005) to assess
180 eddy characteristics of the Peru Current System. Halo et al. (2014) used the method
181 for an eddy census of the Mozambique Channel and provided the method as a Matlab
182 toolbox, which was implemented for this study.

183

184 Halo et al. (2014) combined a geometry approach with a dynamic criterion. The
185 former method detected closed SSHa loops (Chelton et al. 2011), whereas the latter
186 involved computing the Okubo-Weiss parameter. The Okubo-Weiss parameter was
187 applied as a criteria or filter to identify regions of vorticity. Negative values beyond a
188 defined negative threshold value were being indicative of a vorticity dominated flow
189 field (Chelton et al. 2007, 2011). Thus, regions within a closed loop of SSHa and
190 characterised by negative vorticity were then typical for the presence of an eddy. The
191 threshold value for the Okubo-Weiss parameter W used by Halo et al. (2014) was W
192 $< 0 \text{ s}^{-2}$. Chelton et al. (2007) applied a value of $W < -2 \times 10^{-12} \text{ s}^{-2}$.

193

194 The parameters values adopted in this study were the following: a maximum radius R_0
195 of 200 km to exclude larger eddies and ocean gyres, a contour interval of 0.002 m to
196 identify closed loops of SSHa, an Okubo-Weiss parameter $W < -2 \times 10^{-12} \text{ s}^{-2}$ as per
197 Chelton et al. (2007) to identify regions of vorticity characterising the flow field, and
198 a Hanning filter that was applied twice to reduce grid scale noise in the computed
199 Okubo-Weiss parameter. The tracking code was limited to identify eddies with radii
200 larger than 22.5 km and a minimum amplitude of 0.02 m. Following an eddy census
201 of the entire domain (Figure 1), eddy statistics were provided for two coastal
202 corridors. These extended eastward from the location of the 100 m depth contour by
203 100 km and 600 km. The western boundary of the each corridor was the coastline,

204 meaning both corridors varied by the width of the continental shelf west of the 100 m
205 depth contours. The shelf is widest just to the south of Fraser Island (Figure 1). The
206 100 km corridor limited the census to eddies that were closest to the coast. These most
207 likely led to the entrainment of near-shore water and subsequent across-shelf transport
208 and observed evidence of entrainment was presented below (section 3.1). The wider
209 corridor of 600 km was used to allow for some limited comparison with Everett et al.
210 (2012) and Pilo et al. (2015).

211

212 The Halo et al. (2014) eddy detection and tracking tool was applied: firstly, to detect
213 eddies, which provided information on mean radius and SSHa; secondly, to track their
214 movements, which provided information about lifetime; and thirdly, to determine
215 their location within the 100 km corridor and a 600 km coastal corridor for
216 comparison with previous studies. A tracked eddy may have entered or left one of the
217 corridors. The number of detected eddies was much larger than the number of tracked
218 individual eddies. A tracked eddy was referred to as an eddy event. It was found that
219 this study utilising the Halo et al. (2014) algorithm identified several important
220 climatological features of the EAC as highlighted by Ridgway and Dunn (2003) and
221 many of the mean eddy characteristics identified in the previous censuses.

222

223 **3. Results**

224

225 The application of the Halo et al. (2014) resulted in an archive of detected eddies and
226 the location of eddy cores at a particular date. Once detected, we then inspected the
227 database of daily Chl-a and SST images for evidence of these eddies in ocean colour.
228 Several examples of identified eddies were presented in Section 3.1 showing the

229 detected eddy core location and remotely sensed Chl-a for the shelf region of
230 southeast Queensland. In Section 3.2, a tracked eddy was presented as an example for
231 all those tracked in the census. The census was described further in Section 3.3 with
232 results being summarised in Table 1 and 2.

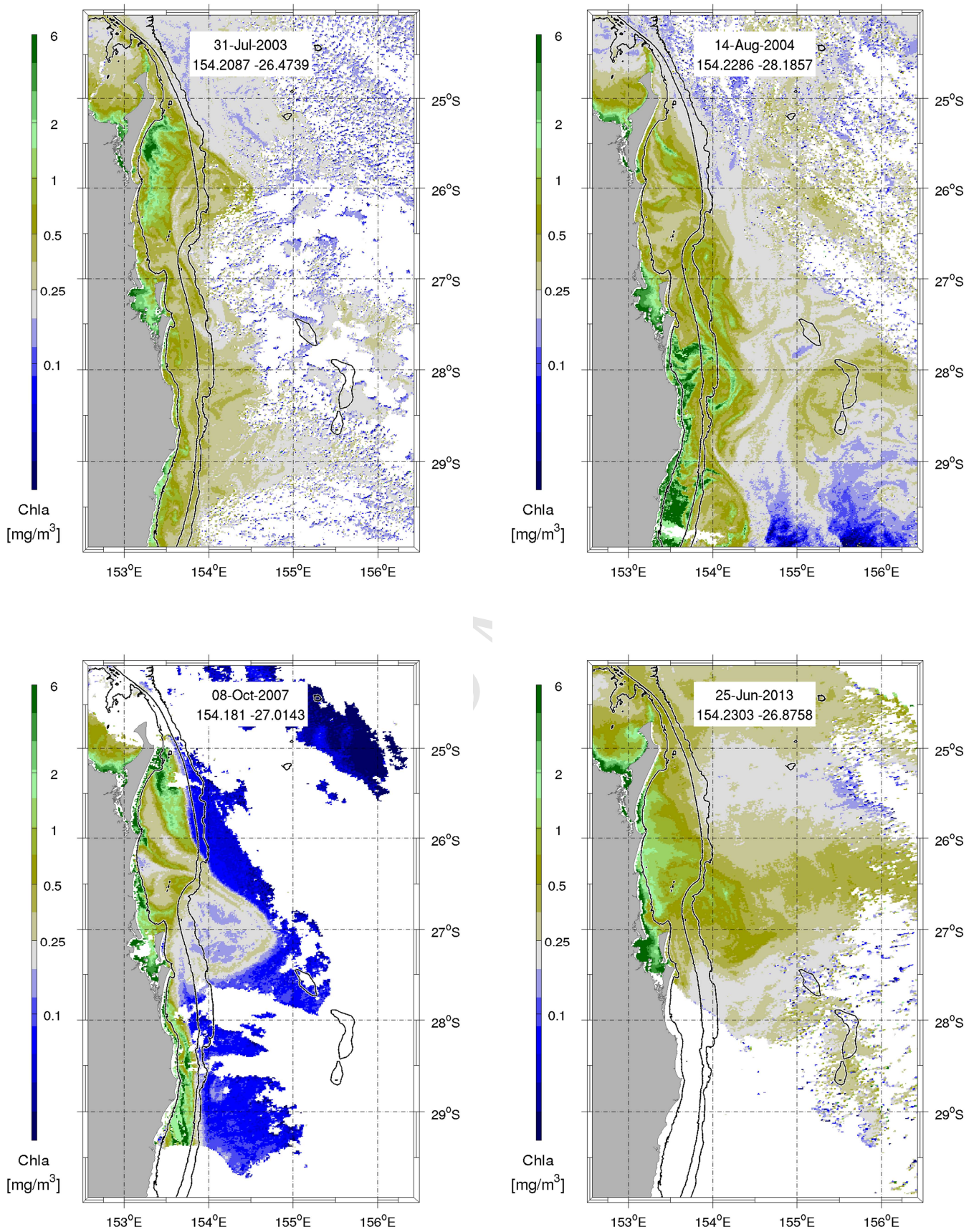
233

234 3.1 Detected individual cyclonic eddies

235

236 The eddy detection tool identified CEs on July 31, 2003 with an eddy core located at
237 154.2087 °E and 26.4739 °S; on August 14, 2004 with an eddy core located at
238 154.2286 °E and 28.1857 °S; on October 8, 2007 with an eddy core located at 154.181
239 °E and 27.0143 °S; and on June 25, 2013 with an eddy core located at 154.2303 °E
240 and 26.8758 °S. CEs and corresponding Chl-a concentrations were shown in Figure 2.

241



242 Figure 2: Series of detected CE with coordinates of detected eddy cores on July 31,
243 2003; August 14, 2004; October 8, 2007 and June 25 2013 indicated and
244 corresponding images of the Chl-a concentration (mg/m^3) on those dates. Indicated
245 are the 40 m, 200 m, and 1000 m depth contours.

246

247 The Chl-a images (Figure 2) were selected following the identification of an eddy
248 core on a particular day. In all cases, the region of the eddy's location was
249 characterised by higher Chl-a concentrations. Elevated Chl-a filaments (e.g. with
250 values of about $6 \text{ mg}/\text{m}^3$ on August 14, 2004) extended away from near coastal waters
251 in a cyclonic fashion across the 40-80 km wide shelf off southeast Queensland. This
252 was indicative of the eddy's interaction with the shallow shelf waters and the
253 entrainment of near coastal high nutrient primary productivity stimulating waters.

254

255 3.2 Tracking a cyclonic eddy

256

257 Chl-a and SST filaments observed for a detected and tracked eddy, indicated that this
258 particular CE interacted with the shallow ($<40 \text{ m}$) near-coast shelf (Figure 3). It
259 exported water off-shore in a cyclonic fashion as evident from entrained water
260 characterised by elevated Chl-a and cooler coastal water.

261

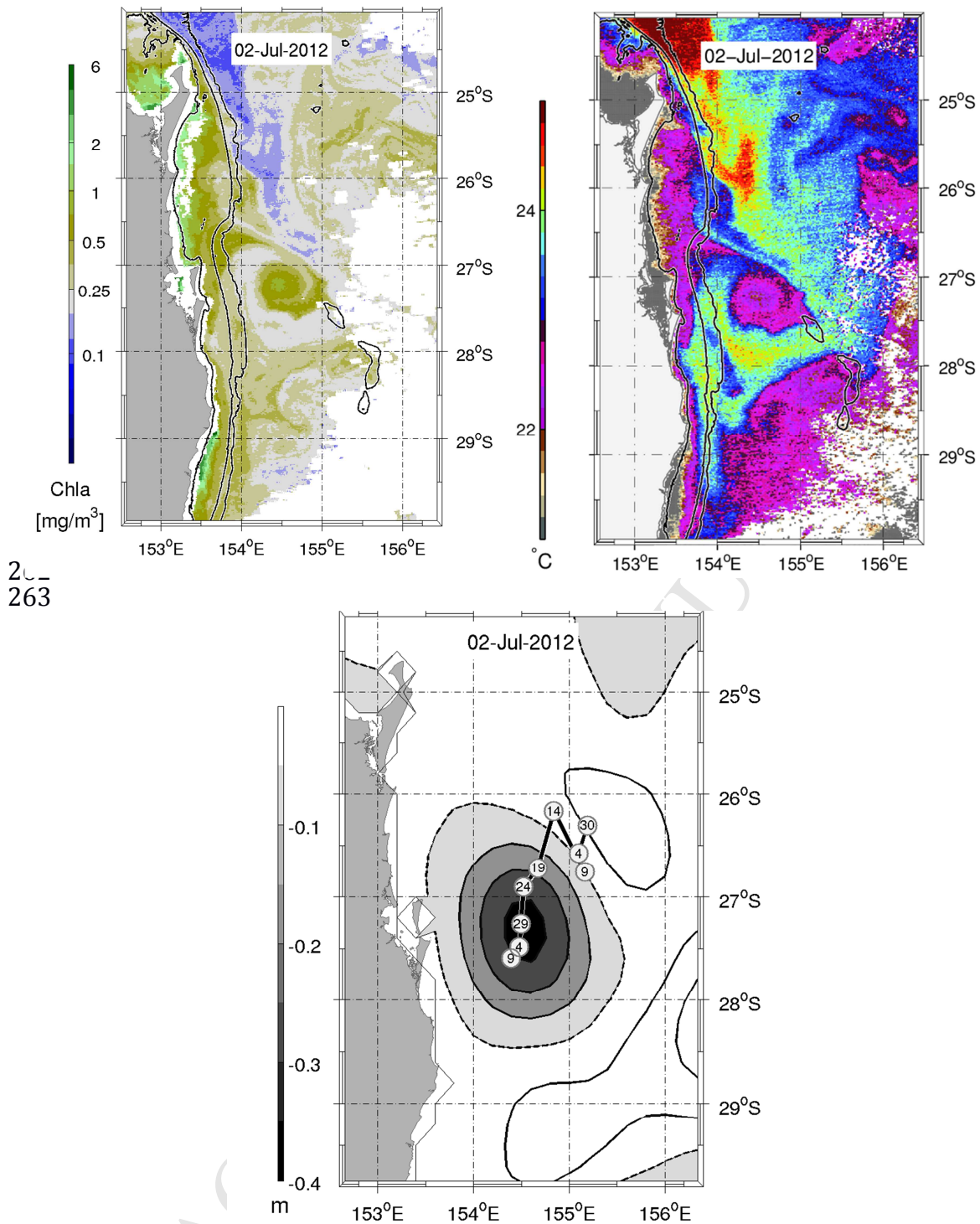


Figure 3: Evidence of a CE detected on July 2, 2012 from remotely sensed (top left panel) Chl-a (mg/m^3), (top right panel) SST ($^{\circ}\text{C}$), and (lower panel) SSHa (m) with negative SSHa anomalies contoured in intervals of 0.05 m. The location of the core of the eddy was traced from its initial detection on May 28 to its dissipation on July 12.

270 Circles in (c) indicate location and date of core with core locations shown for May 30,
271 June 4-29 and finally for July 9, 2012.

272

273 The CE appeared to be wedged between the shelf break and the EAC. The core of the
274 CE was situated at about 154.5 °E. The EAC was evident from the higher SST (>25
275 °C) emerging in the north and extending southward along the shelf break and was
276 associated with lower Chl-a concentrations (Figure 3). The CE appeared to deflect the
277 EAC flow eastward.

278

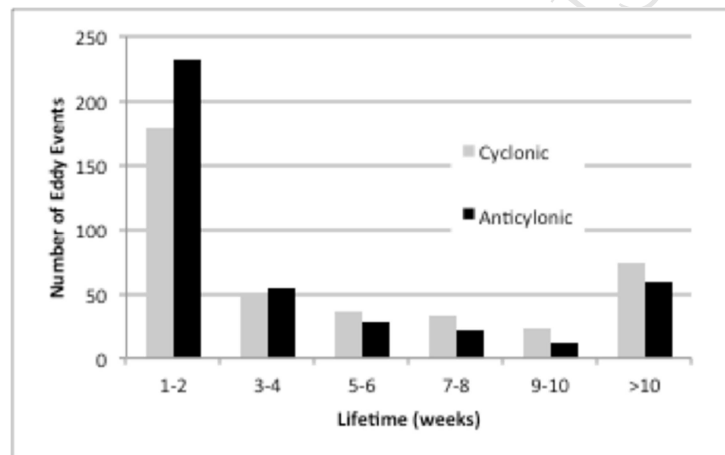
279 First identified on May 28th, 2012, the eddy was initially located at about 155.2 °E and
280 26.3 °S or about 150 km to the northeast of its location on July 2, 2012. Its radius was
281 about 46 km, covering a surface area of 6642 km² and extended westward close to the
282 coast with SSHa at about -0.05 m. The eddy was tracked over a period of about six
283 weeks (Figure 3 with core locations indicated). After a maximum in SSHa of about -
284 0.2 m on July 2, 2012 at location 154.5 °E and 27.25 °S, the CE started to rapidly
285 decay. It had dissipated by about July 11, 2012 with SSHa of less than 0.05 m and
286 reached a most southern location of 154.4°E and 27.5 °S. Its mean latitudinal
287 displacement speed in a south-westerly direction from about 26.3 °S to about 27.3 °S
288 (~110 km) over the six week period was estimated with about ~3 km per day. This
289 displacement speed was similar to the mean speed of 3.2 km per day identified by Pilo
290 et al. (2015) for CEs from the Chelton et al (2011) eddy census. It was representative
291 for the mean displacement speeds (~4 km per day) found for all CE detected in this
292 study. On July 2, 2012, the SST anomaly was about -0.9 °C and the Chl-a eddy core
293 concentration was about 1 mg/m³ and above a typical background level of about 0.2
294 mg/m³. The maximum SSHa was about -0.2 m (Figure 2c).

295 3.3 The East Australian Current Eddy Census

296

297 The number of all tracked eddy events across the region (see Figure 1) with lifetime
 298 of at least 1-2 weeks was 804 (Figure 4). This included 395 CEs (49%) and 409 ACEs
 299 (51%). There were on average about 37 eddy events per year. Short-lived eddies
 300 (lifetime 7-28 days) contributed about 64% of all tracked eddies. Eddies lasting more
 301 than 10 weeks made up 16% of the total and potentially exited from the area
 302 considered in this study.

303



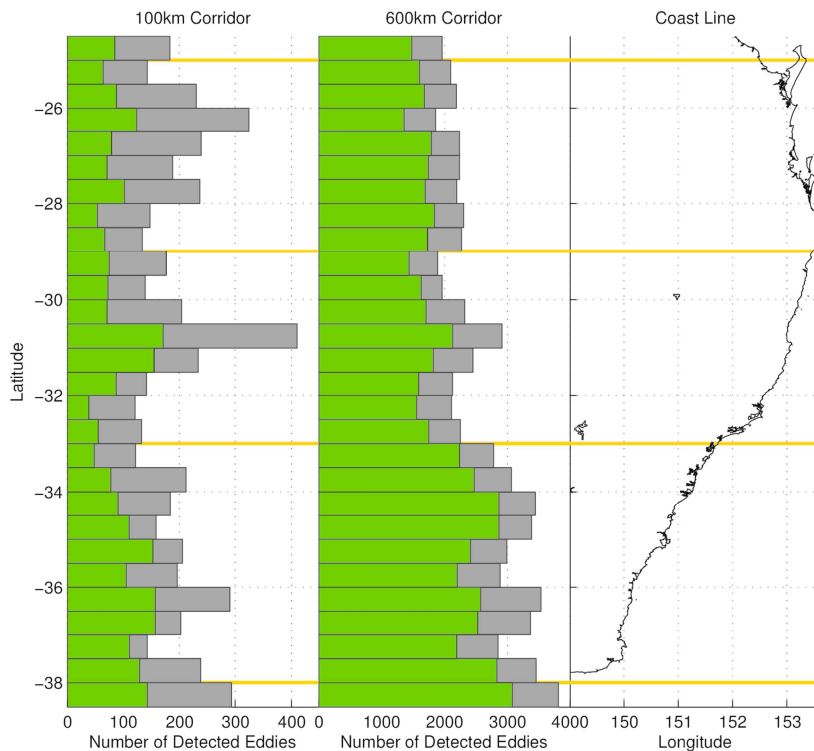
304

305 Figure 4: Lifetime (weeks) of CE and ACE during the period 1993 to 2015.

306

307 The total number of detected eddies per degree latitude was shown for both the 100
 308 km and 600 km wide coastal corridors and for detected eddies with lifetime >7 days
 309 and >28 days (Figure 5). The distribution of detected CEs and ACEs per degree
 310 latitudes was represented in Figure 6.

311



312

313

314 Figure 5: Eddy census for the period 1993-2015 and coastal corridors of 100 km (left

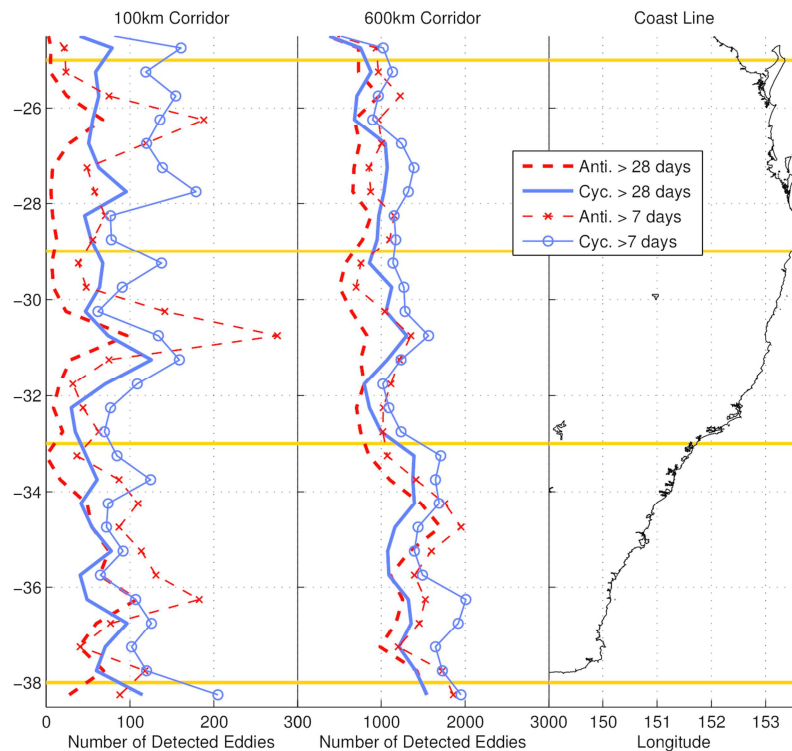
315 panel) and 600 km (right panel) width. Shown is the total number of detected eddies

316 per degree latitude for eddies with lifetime > 7 days (light grey) and > 28 days (green).

317 The right hand panel shows the coast and horizontal lines were shown to coincide

318 with minima in eddy activity, which result in distinguishing between the three zones.

319



320

321

322 Figure 6: Total number of detected ACE (dashed lines) and CE (solid lines) shown for
 323 both 7 days and 28 days lifetime.

324

325 The number of detected short-lived (7-28 days) eddies and tracked eddy events (Table
 326 1) followed from the difference between eddies lasting at least 7 days and those
 327 lasting more than 28 days. For example, in the case of the 600 km wide corridor, the
 328 number of total detected CEs and ACEs was at a maximum within Z3 (Table 1).

329 About 67273 detected eddies ($\Sigma 1$ with 35805 plus $\Sigma 2$ with 31468) were identified that
 330 lasted at least 7 days and of those, 52300 ($\Sigma 1$ with 28211 plus $\Sigma 2$ with 24089) lasted
 331 28 days and longer. Therefore, about 14973 detected eddies were short-lived (7-28
 332 days) within the 600 km corridor of Z3.

333

334 Short-lived detected ACEs (7-28 days) dominated the 100 km coastal corridor and
335 contributed about 64% of all detected ACEs along the EAC. In contrast, only about
336 23% of all detected ACEs were short-lived within the 600 km wide coastal corridor.
337 This followed from an evaluation of the data presented in Table 1. The total number
338 of detected ACEs with lifetime of more than 7 days was 2554 (Σ 2, 100 km) and
339 31468 (Σ 2, 600 km). Of those, 1645 detected eddies or 64% in the 100 km corridor
340 and 7379 detected eddies or about 23 % in the 600 km corridor were short-lived.

341

342 Short-lived (7-28 days) detected eddies (CEs and ACEs) dominated the northern zone
343 (Z1) of the 100 km corridor. The total number of all detected short-lived eddies was
344 994 in Z1 (Table 1: 515 CEs and 479 ACEs) from a total of all detected eddies (>7
345 days) of 1643 (Table 1: 1003 CEs and 640 ACEs). This corresponded to a total of 202
346 short-lived eddy events or 41% in Z1 (Table 1: 94 CEs plus 108 ACEs), 154 short-
347 lived eddy events or 31% in Z2 (Table 1: 57 CEs plus 97 ACEs), and 141 short-lived
348 eddy events or 28% in Z3 (Table 1: 70 CEs plus 71 ACEs). In other words, of the
349 total number of 497 short-lived eddy events tracked within the 100 km corridor (Σ 1 =
350 221 CE events plus Σ 2 = 276 ACE events), Z1, Z2 and Z3 each contributed 41%,
351 31%, and 28 % of short-lived eddy events respectively.

352

353

354 **Table 1**

355 Number of detected eddies and tracked eddies for both EAC corridors

356

100 km corridor	C□□□□□□□				□□□□□□□□□□			
	Z1	Z2	Z3	Σ□	Z1	Z2	Z3	Σ□
Life-time > 7 days								
Detected eddies	1003	840	1264	3107	640	719	1195	2554
Eddy events	153	121	151	425	138	127	150	415
Life-time > 28 days								
Detected eddies	488	515	602	1605	161	211	537	909
Eddy events	59	64	81	204	30	30	79	139
Life-time 7-28 days								
Detected eddies	515	325	662	1502	479	508	658	1645
Eddy events	94	57	70	221	108	97	71	276
600 km corridor								
Life-time > 7 days								
Detected eddies	9277	9840	16688	35805	8148	8218	15102	31468
Eddy events	585	590	1011	2186	616	628	762	2006
Life-time > 28 days								
Detected eddies	7340	8077	12794	28211	6110	5551	12428	24089
Eddy events	266	309	438	1013	268	245	393	906
Life-time 7-28 days								
Detected eddies	1937	1763	3894	7594	2038	2667	2674	7379
Eddy events	319	281	573	1173	348	383	369	1100

357

358

359

360 The Halo et al. (2014) detection and tracking tool appeared to have also captured the

361 approximate location of the centre of two quasi-permanent anticyclonic EAC

362 recirculation cells that were identified previously by Ridgeway and Dunn (2003, their

363 Figure 7). This was evident from two maxima in detected ACEs at about 26°S and

364 31°S (Figure 6). The latter maximum was also evident in the total of all detected

365 eddies (Figure 5) and found to be close to the approximate location of the EAC

366 separation point. It further vindicated the use of Halo et al. (2014) as an appropriate

367 tool to detect and track eddies.

368

369 The northern zone Z1 off the coast of southeast Queensland was characterised by the

370 largest number of tracked short-lived CE events (94 or 43% of the total of 221 tracked

371 eddy events) within the 100 km wide coastal corridor (Table 1). Z1 was part of the
372 previously identified EAC intensification zone (Ridgway and Dunn 2003).

373

374 The total number of detected ACEs in the 100 km wide corridor and with lifetime > 7
375 days was found to be about 2554 (Table 1). The number of detected ACEs per zone
376 increased north to south from 25% (640 detected eddies in Z1) and 28% (719 detected
377 eddies in Z2) to a maximum of 47% (1195 detected eddies in Z3) (in Table 1) south
378 of about 33°S (Z3) and within the EAC separation zone where the EAC's eastward
379 flow eastward is often associated with the spawning long-lasting anticyclonic eddies
380 (e.g. Nielson and Cresswell 1981).

381

382 The identified minima in the latitudinal distribution of detected eddies located at
383 about 29° S and 33° S (see Figure 5 and Figure 6) divided the east Australian coast
384 into three discernible zones. These zones were previously distinguished based on the
385 mean EAC characteristics by Ridgway and Dunn (2003) and referred to as the
386 intensification (Z1, north of about 29 °S) and separation zone (combined Z2 and Z3,
387 south of about 29 °S), which includes the location of the EAC separation point and
388 where the EAC turns toward the east. In the northern region Z1 and within the 100 km
389 wide coastal corridor, the total number of short-lived (7-28 days) tracked CEs and
390 ACEs was found to be highest. The southern boundary of Z1 was evident from a
391 minimum in eddy activity located at 29 °S coinciding with the approximate southern
392 boundary of the EAC intensification zone (Ridgway and Dunn 2003).

393

394 The combined two southern zones Z2 and Z3 comprised the EAC separation zone
395 (Ridgway and Dunn 2003). The southern boundary between both zones was found to

396 coincide with the approximate location of the EAC separation point (30 °S or 31 °S to
397 34 °S, e.g. Godfrey et al. 1980; Ridgway and Dunn 2003) and where EAC turns
398 toward the east between about 33-35 °S (Ridgway and Dunn 2003) and into the
399 Tasman Sea. The number of eddies detected in both the 100 km and particular the 600
400 km wide corridors increased south of about 33 °S and the boundary between zones Z2
401 and Z3, which is within the region where the EAC separates from the coast. This
402 finding was consistent with previous findings (Everett et al. 2012).

403

404 The number of detected and tracked eddies lasting at least four weeks was compared
405 with the Everett et al. (2012) and Pilo et al. (2015), noting that Everett et al. (2012)
406 only reported detected eddies and individual eddies were not tracked.

407

408 Everett et al. (2012) reported 50.2% CEs and 49.8% ACEs from a total of 2613
409 detected eddies for “Eddy Avenue”. In this study, Z2 and Z3 combined (100 km
410 corridor) were broadly part of the “Eddy Avenue”, which found 59.89% CEs and
411 40.10% ACEs from a total of 1865 detected eddies (i.e. 515+602+211+537; Table 1,
412 >28 days). The total number of detected eddies was about 1/3 less than that reported
413 by Everett et al. (2012), who reported 1314 CEs (this study 1117 CEs) and 1299
414 ACEs (this study 748 ACEs). Everett et al. (2012) and this study found agreement in
415 the tendencies for the total number of detected eddies to increase significantly for the
416 larger Tasman Sea area. Everett et al. (2012) reported a total of 14094 CEs and 14892
417 ACEs, this study found a total of 28211 CEs and 24089 ACEs (Table 1, >28 days,
418 600 km corridor).

419

420 Pilo et al. (2015) identified a total of 1050 individually tracked eddies (51% CEs, 49%
421 ACEs, lifetime >28 days) or 50 on average per year. This study found to a total of
422 1919 individually tracked eddies (Σ 1013 plus Σ 2 906, see Table 1, >28 days, 600
423 km corridor) or about 87 on average per year (53 % CEs, 47 % ACEs, see Table 1,
424 >28 days, 600 km corridor). In both studies more CEs than ACEs were tracked.

425

426 Mean characteristics quantified for detected eddies within the 100 km wide coastal
427 corridor appeared to be consistent with the conventional eddy model (e.g. Bakun
428 2006; Everett et al. 2012; Weeks et al. 2010) with mean Chl-a high for CEs than
429 ACEs. The model postulates that CEs are to be associated with higher Chl-a due to
430 upwelling that supplies primary productivity enhancing nutrient rich water to the
431 surface, while ACE characterised by lower Chl-a. Yet, inspection of satellite imagery
432 (Figure 2 and 3) indicated that SST and Chl-a core characteristics identified in this
433 study were likely to be a significantly controlled by the entrainment of coastal waters
434 and potential entrainment from other depths. Everett et al. (2012) also found and
435 discussed a significant departure of mean SST and Chl-a characteristics from the
436 conventional eddy model. In this study, mean SSHa was negative for detected CEs
437 and positive for ACEs (Table 2). Detected CEs had lower mean SST and higher mean
438 Chl-a compared to detected ACEs (22.5 °C vs 22.7 °C and 0.27 mg/m³ vs 0.17 mg/m³,
439 see Table 2), which appeared to be consistent with the standard model, but was
440 potentially contributed to by significant entrainment (Figure 2).

441

442 There appeared to be no discernable difference in mean eddy radii between CEs and
443 ACEs found for all zones (Table 2). Mean radii determined in this study were smaller
444 than those reported by Everett et al. (2012) and Pilo et al. (2015) who reported 92 km

445 and 83.4 km radii for CEs and 95 km and 82.5 km for ACEs 95 km respectively.
 446 These previous studies were based on eddies with lifetime >28 days and mean radii
 447 larger than 40 km (Chelton et al 2011). This study's minimum detected eddy radius
 448 was 22.5 km. Rotational speeds (~0.4 m/s to 0.5 m/s) and mean displacement speeds
 449 (about 0.05 m/s or about 4 km/day) were similar to values reported by Everett et al.
 450 (2012) and Pilo et al. (2015). Considering an estimated mean displacement speed of
 451 the 4 km/day and a lifetime of 7-28 days, a short-lived eddy potentially travelled a
 452 distance of about 115 km. This mean value based on the tracking tool was found to be
 453 similar to the value estimated from tracking the individual eddy shown in Figure 3.
 454 Mean core characteristics SST and Chl-a displayed no discernable difference between
 455 CEs and ACEs (Table 2) Anomalies for both were found to be very small (not
 456 shown). This was likely due to the entrainment process of coastal water, which was
 457 likely associated with high Chl-a and low SST filaments near the edge of the eddy,
 458 which appeared to emanate from the near shore shelf waters as apparent from
 459 inspection of Figure 3 and Figure 4.

460

461 **Table 2**

462 Mean cyclonic and anticyclonic eddy characteristics for the 100 km wide coastal corridor,
 463 individual zones Z1 to Z2 and the average of all zones.

464

Eddy Characteristics	Cyclonic Eddies			Anticyclonic Eddies		
	Z1	Z2	Z3	Z1	Z2	Z3
Life-time > 7 days						
Radius (10^3 m)	60±14	57±14	52±12	55±12	53±13	53±14
SSHa (10^{-2} m)	-12±9	-17±11	-12±8	10±6	17±10	19±13
Rotational Speed (10^{-2} m/s)	44±22	53±23	47±23	29±12	35±16	50±25
Chl-a (mg/m^3)	0.18±0.13	0.22±0.12	0.43±0.36	0.11±0.08	0.14±0.09	0.26±0.78
SST ($^{\circ}\text{C}$)	24.08±1.98	23.13±2.17	20.24±2.38	24.63±1.77	23.03±1.93	20.45±2.12
Radius (10^3 m)	66±13	62±13	55±11	61±14	56±13	60±13
SSHa (10^{-2} m)	-16±10	-19±11	-14±8	12±6	17±10	24±13
Rotational Speed (10^{-2} m/s)	52±24	60±23	52±23	35±13	37±16	63±25
Chl-a (mg/m^3)	0.22±0.15	0.23±0.12	0.44±0.42	0.11±0.1	0.1±0.08	0.2±0.12
SST ($^{\circ}\text{C}$)	24.14±2.3	23±2.2	20.36±2.4	24.15±1.6	23.91±2.1	20.34±1.9

465

466 4. Discussion and Conclusion

467

468 The latitudinal location with maxima in detected ACEs at about 26°S and 31°S was
469 found to be consistent with the climatological location of two centres of previously
470 identified EAC anticyclonic recirculation cells (Ridgway and Dunn 2003). The
471 location of the EAC separation point at about 31.5 °S was evident from the maximum
472 of detected eddies between 30 °S and 31 °S (Figure 5 and Figure 6). Here, the
473 separation of the EAC from the coast alleviates the restriction for ACEs formation
474 and the number of detected ACEs increased again southward of 33 °S (Figure 6). This
475 was found to be consistent with other studies (Everett et al. 2012, Piolo et al. 2015).
476 The increase was more apparent for the 600 km corridor where the most southern
477 zone Z3 was characterised by the highest number of detected eddies (Figure 5).

478

479 In the northern zone Z1 off the coast of southeast Queensland, both short-lived (7-28
480 days) CE and ACE events were found to be dominant within the 100 km wide
481 corridor (Table 1). Mean eddy characteristics such as radii, SSHa, SST, Chl-a and
482 total number of detected eddies confirmed with the conventional eddy model and
483 were found to be broadly consistent with those derived from the Chelton et al. (2011)
484 data base (Everett et al. 2012, Pilo et al.2015). Dissimilarities were expected due to
485 different detection and tracking tools, SSHa temporal resolution, the actual regions
486 analysed, different minimum radii applied and minimum lifetime of eddies considered
487 (i.e. 7-28 days versus >28 days in previous studies). The eddy census based on the
488 Halo et al. (2014) method was broadly in good agreement with that from Chelton et
489 al. (2011) for the same coastal domain between total number of detected eddies, but

490 some differences in their distribution. The comparison also identified the two maxima
491 in detected eddies at 27°S and 31°S in the Chelton et al. (2011) database.

492

493 The continental shelf off southeast Queensland and to the south of Fraser Island was
494 found to be home to about 43% of all short-lived detected CEs within a 100 km
495 coastal corridor along the east Australian coast. This corresponded to a total of 94
496 individual CE events tracked during the period 1993-2015 or about 4-5 CEs on
497 average per year. These CEs were likely to encroach onto the shelf leading to the
498 entrainment of near shore water and across-shelf transport as discussed for several
499 individual events (Figure 2 and Figure 3). The frequent occurrence of these CEs could
500 likely contribute to establishing a quasi-permanent alongshore near coast northward
501 flow as it was observed for the separation zone of the EAC (Huyer et al. 1988,
502 Roughen et al. 2011). This potentially established a quasi-permanent cyclonic on-
503 shelf EAC recirculation cell south of Fraser Island referred to as the Fraser Island
504 Gyre. The cyclonic on shelf circulation is similar to that of other continental shelf
505 regions characterised by transient CE genesis such as the Charleston Gyre (Govoni et
506 al. 2009). The continuous, but transient throughout the year, entrainment
507 characteristic of the short-lived CEs generated in this region was likely to be part of
508 the enhancement of primary productivity in this region, which was in part also driven
509 by the Southeast Fraser Island Upwelling System (Brieva et al. 2015). The transient
510 eddies were likely to transport in a cyclonic fashion fish larvae across the shelf that
511 were subsequently transported to the southern temperate waters of the Tasman Sea by
512 the EAC. This mechanism was postulated by Ward et al. (2003) and this study
513 identified the possible role of CEs and the existence of a quasi-permanent gyre in
514 contributing to the cross-shelf exchange process.

515

516 Previous studies of EAC eddy generation and their role in ecosystem dynamics
517 focused on the coastal ocean of New South Wales and the separation zone of the EAC
518 (e.g. Suthers et al. 2011). Results presented here were from an eddy characterisation
519 study with some focus on the coast off southeast Queensland finding that CEs
520 appeared to be a distinct and most prominent feature for this region of the eastern
521 Australian coast. It is noted that this eddy study may have underestimated the
522 presence of CEs for this (and other) region since it is difficult to capture smaller-scale
523 CEs in satellite derived SSHa with a spatial resolution of 22.5 km (see e.g. Macdonald
524 et al. 2016). In the future, it would be prudent to investigate the on-shelf flow pattern
525 and the role of the EAC in this region from in-situ observations augmented with
526 detailed higher resolution modelling studies to confirm the apparent dominant role
527 played by CEs gleaned here from remote sensing data.

528

529 In the case of the EAC, we found that it is the northern EAC intensification zone that
530 was dominated by short-lived CEs (7-28 days). These provided a possible key
531 cyclonic and cross shelf transport mechanism for fish larvae, which is a poorly
532 understood physical process of biological significance (Ward et al. 2003, Mullaney et
533 al. 2013, Mullaney et al. 2014). Frequent CEs of the EAC intensification zone were
534 likely to lead to an alongshore-northerly flow as also documented for the southern
535 EAC separation zone (e.g. Roughen et al. 2011). Combined with a southward flowing
536 EAC along the shelf-break, this would establish an on-shelf characteristic mean
537 oceanographic circulation feature referred to as the Fraser Island Gyre.

538

539

540 **Acknowledgement**

541

542 The authors would like to thank Halo et al. (2014) and colleagues at the Nansen-Tutu
543 Centre for Marine Environmental Research Department of Oceanography, University
544 of Cape Town for access to the eddy detection and tracking tool and colleagues with
545 the Integrated Marine Ocean Observing (IMOS) for providing remote sensing data.
546 Results reported here contributed to a postgraduate research project and Mr Daniel
547 Brieva is thankful to the Chilean Government for providing a scholarship. The
548 authors wish to also acknowledge the constructive feedback that was received from all
549 reviewers, which helped greatly to improve this paper.

550

551 **References**

552

553 Bakun, A., 2006. Fronts and eddies as key structures in the habitat of marine fish
554 larvae: opportunity, adaptive response and competitive advantage. *Scientia Marina* 70,
555 105-122.

556

557 Brieva, D., Ribbe, J., Lemckert, C., 2015. Is the East Australian Current Causing A
558 Marine Ecological Hot Spot and An Important Fisheries near Fraser Island, Australia?
559 *Estuarine, Coastal and Shelf Science* 153, 121-134, doi: 10.1016/j.ecss.2014.12.012.

560

561 Chelton, D. B., Schlax, M. G., Samelson, R. M., de Szoeke, R. A., 2007. Global
562 observations of large oceanic eddies. *Geophysical Research Letters* 34, L15606, doi:
563 10.1029/2007gl030812.

564

- 565 Chelton, D. B., Schlax, M.G., Samelson, R.M., 2011. Global observations of
566 nonlinear mesoscale eddies. *Progress in Oceanography* 91, 167–216.
567
- 568 Claustre, H., Maritorena, S., 2003. The Many Shades of Ocean Blue. *Science* 302,
569 1514–1515.
570
- 571 Everett, J. D., Baird, M. E., Suthers, I. M., 2011. Three-dimensional structure of a
572 swarm of the salp *Thalia democratica* within a cold-core eddy off southeast Australia.
573 *Journal of Geophysical Research – Ocean* 116, C12046.
574
- 575 Everett, J. D., Baird, M. E., Oke, P. R., Suthers, I. M., 2012. An avenue of eddies:
576 Quantifying the biophysical properties of mesoscale eddies in the Tasman Sea.
577 *Geophysical Research Letters* 39, doi: 10.1029/2012GL053091.
578
- 579 Everett, J. D., Baird, M. E., Roughan, M., Suthers, I. M., Doblin, M. A., 2014.
580 Relative impact of seasonal and oceanographic drivers on surface chlorophyll a along
581 a Western Boundary Current. *Progress in Oceanography* 120, 340-351.
582
- 583 Everett, J. D., Macdonald, H., Baird, M. E., Humphries, J., Roughan, M., Suthers, I.
584 M., 2015. Cyclonic entrainment of preconditioned shelf waters into a frontal eddy.
585 *Journal of Geophysical Research – Ocean* 120, doi: 10.1002/2014JC01301.
586
- 587 Godfrey, J. S., Cresswell, G. R., Golding, T. J., Pearce, A. F., 1980. The Separation of
588 the East Australian Current. *Journal of Physical Oceanography* 10, 430-440.
589

- 590 Govoni, J. J., Hare, J. A., Davenport, E. D., Chen, M. H., Marancik, K. E., 2009.
591 Mescoscale, cyclonic eddies as larval fish habitat along the southeast United States
592 shelf: a Lagrangian description of the zooplankton community. *ICES Journal of*
593 *Marine Science* 67, 403-411.
594
- 595 Gruber, N., Lachkar, Z., Frenzel, H., Marchesiello, P., Munnich, M., McWilliams, J.
596 C., Nagai, T., Plattner, G.-K., 2011. Eddy-induced reduction of biological production
597 in eastern boundary upwelling systems. *Nature Geoscience* 4, 787-792.
598
- 599 Halo, I., Backeberg, B., Penven, P., Ansorge, I., Reason, C., Ullgren, J. E., 2014.
600 Eddy properties in the Mozambique Channel: A comparison between observations
601 and two numerical ocean circulation models. *Deep Sea Research Part II: Topical*
602 *Studies in Oceanography* 100, 38-53.
603
- 604 Henson, S. A., Thomas, A. C., 2008. A census of oceanic anticyclonic eddies in the
605 Gulf of Alaska. *Deep-Sea Research Part I: Oceanographic Research Papers* 55, 163-
606 176.
607
- 608 Huyer, A., Smith, R. L., Stabeno, P. J., Church, J. A., White, N. J., 1988. Currents of
609 South-eastern Australia: Results from the Australian Coastal Experiment. *Australian*
610 *Journal of Marine and Freshwater Research* 39, 245-288.
611
- 612 IMOS, 2015a. Chlorophyll-a concentration (OC3) (Last access November 2015).
613 <http://rs-data1-mel.csiro.au/thredds/catalog/imos-srs/oc/aqua/1d/catalog.html>
614

- 615 IMOS, 2015b. Gridded sea level anomaly (Last access November 2015).
616 [http://thredds.aodn.org.au/thredds/catalog/IMOS/OceanCurrent/GSLA/DM00/catalog.](http://thredds.aodn.org.au/thredds/catalog/IMOS/OceanCurrent/GSLA/DM00/catalog.html)
617 [html](#)
618
- 619 Karstensen, J., Fiedler, B., Schütte, F., Brandt, P., Körtzinger, A., Fischer, G.,
620 Zantopp, R., Hahn, J., Visbeck, M., Wallace, D., 2015. Open ocean dead zones in the
621 tropical North Atlantic Ocean. *Biogeosciences* 12, 2597-2605.
622
- 623 Kasai, A., Kimura, S., Nakata, H., Okazaki, Y., 2002. Entrainment of coastal water
624 into a frontal eddy of the Kuroshio and its biological significance. *Journal of Marine*
625 *Systems* 37, 185-198.
626
- 627 Macdonald, H. S., Roughan, M., Baird, M., Wilkin, J., 2016. The formation of a cold-
628 core eddy in the East Australian Current. *Continental Shelf Research* 114, 72-84.
629
- 630 Mason, E., Pascual, A., McWilliams, J. C., 2014. A New Sea Surface Height–Based
631 Code for Oceanic Mesoscale Eddy Tracking. *Journal of Atmospheric and Oceanic*
632 *Technology* 31, 1181–1188, doi: 10.1175/JTECH-D-14-00019.1.
633
- 634 Matis, P. A., Figueira, W. F., Suthers, I. M., Humphries, J., Miskiewicz, A., Coleman
635 R. A., Kelaher, B. P., Taylor, M. D., 2014. Cyclonic entrainment? The
636 ichthyoplankton attributes of three major water mass types generated by the
637 separation of the East Australian Current. *ICES Journal of Marine Science* 71, 1696-
638 1705, doi: 10.1093/icesjms/fsu062.
639

- 640 Morrow, R., Le Traon, P.-Y., 2012. Recent advances in observing mesoscale ocean
641 dynamics with satellite altimetry. *Advances in Space Research* 50, 1062-1076.
642
- 643 Mullaney, T. J., Suthers, I. M., 2013. Entrainment and retention of the coastal larval
644 fish assemblage by a short-lived, submesoscale, frontal eddy of the East Australian
645 Current. *Limnology and Oceanography* 56, 1546-1556.
646
- 647 Mullaney, T. J., Gillanders, B. M., Heagney, E. C., Suthers, I. M., 2014. Entrainment
648 and advection of larval sardine, *Sardinops sagax*, by the East Australian Current and
649 retention in the western Tasman Front. *Fisheries Oceanography* 23, 554-567.
650
- 651 Nilsson, C. S., Cresswell, G. R., 1981. The formation and evolution of East Australian
652 Current warm-core eddies. *Progress in Oceanography* 9, 133-183.
653
- 654 Oke, P., Griffin, D., 2010. The cold-core eddy and strong upwelling off the coast of
655 new South Wales in early 2007. *Deep Sea Research Part II: Topical Studies in*
656 *Oceanography* 58, 574-591.
657
- 658 O'Reilly, J.E. et al., 2000. SeaWiFS Post Launch Calibration and Validation
659 Analyses, Part 3. In: Hooker s. B., firestone, E. R. (Eds.), *NASA Tech. Memo. 2000-*
660 *206892*, NASA Goddard Space Flight Center, vol. 11, 49 pp.
661
- 662 Pegliasco, C, Chaigneau, A., Morrow, R., 2015. Main eddy vertical structures
663 observed in the four Eastern Boundary Upwelling Systems. *Journal of Geophysical*
664 *Research – Oceans* 120, doi: 10.1002/2015JC010950.

665

666 Penven, P., Échevin, V., Pasopera, J., Colas, F., Tam, J., 2005. Average circulation,
667 seasonal cycle and mesoscale dynamics of the Peru Current System: a modelling
668 approach. *Journal of Geophysical Research - Ocean* 110, C10021.

669

670 Pilo, G. S., Mata, M. M., Azevedo, J. L. L., 2015. Eddy Surface properties and
671 propagation at Southern Hemisphere western boundary current systems. *Ocean*
672 *Science Discussions* 12, 135-160.

673

674 Ridgway, K. R., Dunn, J. R., 2003. Mesoscale structure of the mean East Australian
675 Current System and its relationship with topography. *Progress in Oceanography* 56,
676 189-222.

677

678 Roughen, M., Macdonald, H. S., Baird, M. E., Glasby, T. M., 2011. Modelling coastal
679 connectivity in a Western Boundary Current: Seasonal and inter-annual variability.
680 *Deep-Sea Research II* 58, 628-644.

681

682 Suthers, I. M., J. W. Young, et al. 2011. The strengthening East Australian Current, its
683 eddies and biological effects — an introduction and overview. *Deep Sea Research*
684 *Part II: Topical Studies in Oceanography* 58, 538-546.

685

686 Weeks, S. J., Bakun, A., Steinberg, C. R., Brinkman, R., Hoegh-Guldberg, O.,
687 2010. The Capricorn Eddy: a prominent driver of the ecology and future of the
688 the southern Great Barrier Reef. *Coral Reefs* 29, 975-985.

689

690 Ward, T. M., Staunton-Smith, J., Hoyle, S., Halliday, I. A., 2003. Spawning patterns
691 of four species of predominantly temperate pelagic fishes in the sub-tropical waters of
692 southern Queensland. Estuarine, Coastal and Shelf Science 56, 1125-1140.

ACCEPTED MANUSCRIPT

693

694 **List of Tables**

695

696 Table 1: Number of detected eddies and tracked eddies for both EAC corridors.

697

698 Table 2: Mean cyclonic and anticyclonic eddy characteristics for the 100 km wide
699 coastal corridor, individual zones Z1 to Z2 and the average of all zones.

700

701

702

703

704 **List of Figures**

705

706 Figure 1: Location of the study site along the east coast of Australia. The
707 boundaries between Zone 1 (Z1) and Zone 2 (Z2) at about 29° S and Z2
708 and Zone 3 (Z3) at about 33° S were identified in this study from minima
709 in eddy activity. Approximate mean path of the East Australian Current
710 (EAC) is shown in light grey. Eddies were tracked over the whole region.
711 An eddy census was conducted and the analysis limited to two coastal
712 corridors of 100 km and 600 km width each (dash lines).

713

714 Figure 2: Series of detected CE with coordinates of detected eddy cores on July 31,
715 2003; August 14, 2004; October 8, 2007 and June 25 2013 indicated and
716 corresponding images of the Chl-a concentration (mg/m^3) on those dates.
717 Indicated are the 40 m, 200 m, and 1000 m depth contours.

718

719 Figure 3: Evidence of a CE detected on July 2, 2012 from remotely sensed (a) Chl-a
720 (mg/m^3), (b) SST ($^{\circ}\text{C}$), and (c) SSHa (m) with negative SSHa anomalies
721 contoured in intervals of 0.05 m. The location of the core of the eddy was
722 traced from its initial detection May 28 to its dissipation on July 12.
723 Circles in (c) indicate location and date of core with core locations shown
724 for May 30, June 4-29 and finally for July 9, 2012.

725

726 Figure 4: Characteristic lifetimes of CE and ACE (in weeks) detected during the
727 period 1993 to 2015.

728

729 Figure 5: Eddy census for the period 1993-2015 and coastal corridors of 100 km
730 (left panel) and 600 km (right panel) width. Shown is the total number of
731 detected eddies per degree latitude for eddies lasting at least 7 days (light
732 grey) and 28 days (green). The right hand panel shows the coast and
733 horizontal lines were shown to coincide with minima in eddy activity,
734 which result in distinguishing between the three zones.

735

736 Figure 6: Total number of detected ACE (dashed lines) and CE (solid lines) per
737 degree latitude and shown for both 7 days and 28 days lifetime

ACCEPTED MANUSCRIPT

- 497 short-lived eddies detected in a coastal corridor off eastern Australia.
- About 23 individual short-lived eddies traced per year.
- 43% of cyclonic eddies (4-5 per year) found off southeast Queensland.
- Cyclonic eddies displaced shelf water by about 110-120 km.
- Cyclonic eddies postulated to establish quasi-permanent northward flow.